Low-temperature thermal properties of yttrium and lutetium dodecaborides

2005 J. Phys.: Condens. Matter 17 5971

(http://iopscience.iop.org/0953-8984/17/38/003)

INSTITUTE OF PHYSICS PUBLISHING JOURNAL OF PHYSICS: CONDENSED MATTER

J. Phys.: Condens. Matter **17** (2005) 5971–5985 doi:10.1088/0953-8984/17/38/003

Low-temperature thermal properties of yttrium and lutetium dodecaborides

A Czopnik[1], N Shitsevalova[1,2,5], V Pluzhnikov[1,3], A Krivchikov[1,3], Yu Paderno[2] and Y Onuki[4]

[1] W Trzebiatowski Institute of Low Temperature and Structure Research of PAS, PO Box 1410, 50-950 Wroclaw, Poland
[2] I Frantsevich Institute for Problems of Materials Science of NASU, 3 Krzhyzhanovsky Street, 03680 Kiev, Ukraine
[3] B Verkin Institute for Low Temperature Physics and Engineering of NASU, 47 Lenin Avenue, Kharkiv 61103, Ukraine
[4] Graduate School of Science, Osaka University, Toyonaka 560-0810, Japan

E-mail: shitz@ipms.kiev.ua and nata_shitz@mail.ru

Received 18 February 2005, in final form 22 May 2005
Published 9 September 2005
Online at stacks.iop.org/JPhysCM/17/5971

Abstract

The heat capacity (C_p) and dilatation (α) of YB_{12} and LuB_{12} are studied. C_p of the zone-melted YB_{12} tricrystal is measured in the range 2.5–70 K, of the zone-melted LuB_{12} single crystal in the range 0.6–70 K, and of the LuB_{12} powder sample in the range 4.3–300 K; α of the zone-melted YB_{12} tricrystal and LuB_{12} single crystals is measured in the range 5–200 K. At low temperatures a negative thermal expansion (NTE) is revealed for both compounds: for YB_{12} at 50–70 K, for LuB_{12} at 10–20 K and 60–130 K. Their high-temperature NTE is a consequence of nearly non-interacting freely oscillating metal ions (Einstein oscillators) in cavities of a simple cubic rigid Debye lattice formed by B_{12} cage units. The Einstein temperatures are ∼254 and ∼164 K, and the Debye temperatures are ∼1040 K and ∼1190 K for YB_{12} and LuB_{12} respectively. The LuB_{12} low-temperature NTE is connected with an induced low-energy defect mode. The YB_{12} superconducting transition has not been detected up to 2.5 K.

1. Introduction

Boron forms refractory dodecaborides (MeB_{12}) with heavy lanthanides from terbium to lutetium, and also with scandium, yttrium, zirconium, uranium. Apart from ScB_{12}, they crystallize in the face-centred cubic UB_{12}-type structure (space group $Fm3m$-O_h^5), which may be considered as a cubic lattice formed by rigid units—B_{12} cubooctahedra—with interstitial metallic atoms accommodated in the octahedral pores among them or as a structure in which

[5] Author to whom any correspondence should be addressed.

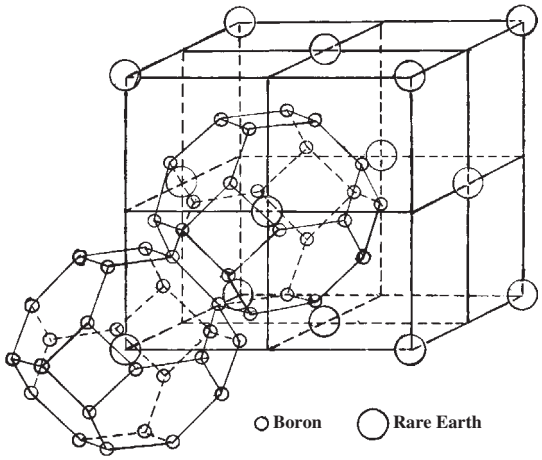

Figure 1. The UB_{12}-type crystal structure of metal dodecaborides.

metallic atoms are located at the centres of the regular Fedorov's cubooctahedra (MeB_{24}) with boron atoms at each their 24 vertices (figure 1).

Strong covalent bonds between boron atoms of inter- and intra-B_{12} cages lead to a very rigid MeB_{12} lattice. The size of the metal atom has a week effect on the unit cell dimension: when the radius of metallic ions is changed from 0.80 to 0.97 Å (∼17%) the unit cell dimension varies from 7.407 to 7.501 Å (∼1.3%) [1]. However, the presence of metal atoms stabilizes this structure and in particular the cubooctahedral form of the B_{12} group due to transferring to the cubooctahedron two valence electrons per metallic atom in order to compensate the electron deficiency in the boron sublattice.

In trivalent metal dodecaborides the third valence electron enters the conduction band that in combination with the rigid MeB_{12} lattice determines their good metal properties. Diamagnetic dodecaborides—ScB_{12}, YB_{12}, ZrB_{12} and LuB_{12}—are superconductors with ordering temperatures of 0.39, 4.7, 5.82 [2] and 0.4 K [3], respectively. Here it is necessary to remark that for YB_{12} the value of $T_c = 4.7$ K in this study has not been confirmed. YbB_{12} belongs to an interesting class of Kondo insulators [4]. The remaining dodecaborides with unfilled 4f-shell are antiferromagnets at low temperatures [5].

At average dimension of the B_{12} cubooctahedron of about 5.35 Å, the radius of the B_{24} cavity changes in the range 1.15–1.2 Å [1]. Taking into account the size of the metal ions it may be supposed that the oscillations of the metal ions (Einstein oscillators) are sufficiently free around their sites, which may result in the appearance of a quasi-local optical mode with the energy inside the Debye spectrum and a deformation of the long-wave range of the spectrum that in its turn has to be reflected in phonon-depending properties. Experimental information on the phonon spectrum of dodecaboride exists only for YbB_{12} [6, 7] and for LuB_{12} [6–9]. It is assumed that their lowest peaks at ∼15.5 and ∼14 meV correspond to the flat mode from non-interacting vibrations of the Me ions while the higher ones are mostly due to the boron optical and rotational modes in the middle energy range and intramolecular B–B vibrations in the highest-energy part.

To shed light on the possible manifestation of such quasi-local optical modes in the crystal properties we have undertaken studies of the thermal properties (heat capacity and thermal expansion) of non-magnetic yttrium and lutetium dodecaborides, which are determined only by the outer electrons and by the phonon spectrum.

The previously published data on the thermal expansion of YB_{12} and LuB_{12} in the temperature range from 78 up to 1200 K show a monotonic increase of the thermal expansion

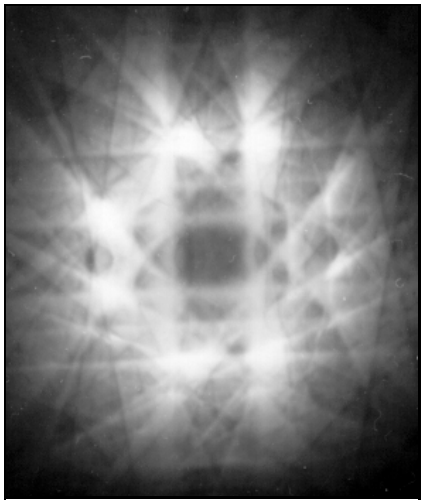

Figure 2. The symmetry electron Kikuchi pattern to the [100] direction for the LuB_{12} single crystal.

coefficient (α) with temperature. These results were obtained using the x-ray method [10, 11] and quartz dilatometers [10, 12] on powders and compact sintered samples. Information on the heat capacity has been reported only for LuB_{12} up to 300 K [4]; its heat capacity is also characterized by a monotonic rise.

Special attention has been paid in this work to the quality of the samples studied.

2. Samples and experimental methods

The process of sample preparation consists of the synthesis of dodecaborides by a borothermal reduction of the metal oxides in vacuum at 1900 K, the compacting of these powders into rods and their subsequent sintering, and of inductive zone melting.

The purity of the initial oxides Y_2O_3 and Lu_2O_3 was 5N and 4N, respectively. The content of the main substance in the initial amorphous boron was no less than 99.5%. Highly volatile impurities in boron were deleted partially during the synthesis procedure and partially during zone melting. The total content of impurities in samples studied was not higher than 10^{-3} mass%.

A part of the LuB_{12} synthesized powder was used for its heat capacity study in the range 4.3–300 K. The composition corresponds to the stoichiometric one; the lattice parameter is equal to 7.4644_2 Å.

The thermal expansion 5–200 K and low-temperature heat capacity (up to 70 K) studies were performed on samples which were cut from the zone-melted YB_{12} tricrystal and on $LuB_{12}\langle 100\rangle$ and $\langle 110\rangle$ single crystals. The lattice parameter of the LuB_{12} single crystal coincides with the powder one due to the rigid boron sublattice; the YB_{12} tricrystal lattice parameter is equal to 7.500_1 Å in accordance with published data [1].

The $\langle 100\rangle$ and $\langle 110\rangle LuB_{12}$ single crystals were grown using correspondingly oriented seeds. According to the x-ray topography and Laue photograph analysis their real structures are highly perfect. Electron diffraction and high-resolution transmission microscopy analysis allowed us to determine the characteristics of local structural details of the single crystals: according to the electron Kikuchi patterns (figure 2) and point electron diffraction patterns (figures 3(a), (b)), which correspond only to the UB_{12}-type structure, defects were practically absent.

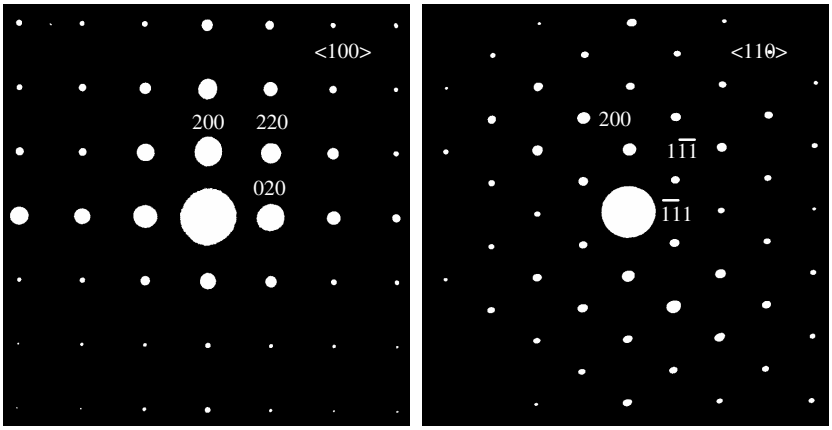

Figure 3. Electron diffraction patterns for two LuB_{12} single crystals along their main zone axes: (a) ⟨100⟩, (b) ⟨110⟩. All reflections correspond to the UB_{12}-type structure.

However, it is impossible to exclude the presence of microdefects in these crystals, as at densities less than 10^6 cm^{-2} the probability of their presence in the area of the visible field is low. A possible existence of defects follows also from the chemical analysis data and the hydrostatic density measurements of the samples. According to them, the composition of the lutetium dodecaboride single crystals may be estimated as $LuB_{11.89\pm0.06}$. Obviously, this composition is at equilibrium for the crystallization temperature. Any attempt to obtain single crystals with a nominal stoichiometry by the input of surplus boron to the initial powders resulted in an instability of the growing process and as a consequence to the obtaining of mosaic crystals.

The yttrium dodecaboride zone-melted sample represented a tricrystal with approximate composition $Y_{0.90}B_{12}$ in agreement with the results of Johnson and Daane [13]: melted yttrium dodecaboride exists only for Y_xB_{12} compositions where $x \leqslant 0.92$. This compound is located on the border of the UB_{12}-type structure stability; therefore the presence of defects in the lattice allows the cubic crystal structure to stabilize.

The heat capacity (C_p) was measured by the pulse quasi-adiabatic method for the YB_{12} tricrystal in the range 2.5–70 K, for the LuB_{12} single crystal in the range 0.6–70 K and for the LuB_{12} powder sample from 4.3 to 300 K using respectively two types of calorimeter (for compact samples and for the powder one) which have been described in detail in [14, 15]. The YB_{12} heat capacity below 6 K was measured also in a magnetic field of 1 T assuming the possibility of the superconductive transition in YB_{12} at 4.7 K [2]. The mass of the LuB_{12} powder sample was about 25 g, and the masses of the zone-melted YB_{12} and LuB_{12} samples were less than 400 mg. The experimental error of the C_p study by a copper standard for the calorimeter with the compact samples is less than 1% in the 0.6 ± 70 K range [14]; in the case of the calorimeter for the powder sample the experimental error compared to a leucosapphire standard is equal to 1.46% in the range 4.3 ± 30 K, 0.53% at 30 ± 100 K, and 0.31% at 100 ± 300 K [15].

The temperature dependence of the relative length change ($\Delta l/l$) was measured by the three-terminal capacitive method in the range 5–200 K with a resolution 1×10^{-9}. The capacitive cell was very similar to the cell described by Brandli and Griessen [16]. The experimental $\Delta l/l$ curves were fitted by a polynomial after subtraction of the experimental cell contribution. The linear thermal expansion coefficient $\alpha = (\partial \ln l/\partial T)_P$ was then

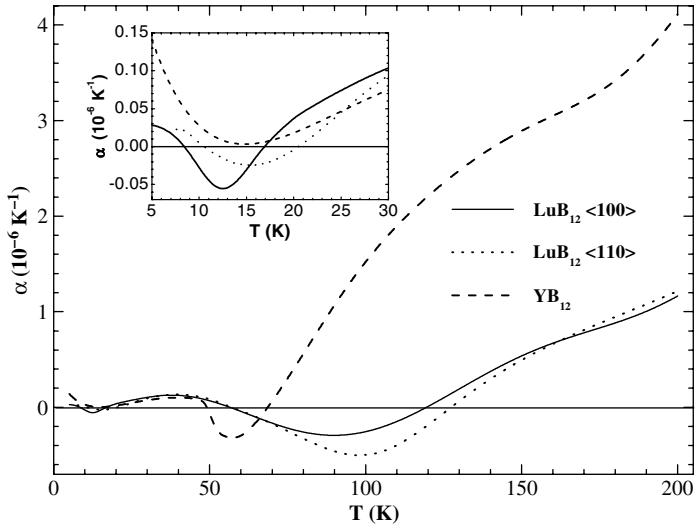

Figure 4. The temperature dependence of the thermal expansion coefficient α for the YB_{12} tricrystal and the $LuB_{12}\langle 100\rangle$ and $\langle 110\rangle$ single crystals. Inset: α versus T in an expanded scale.

determined by differentiating the polynomial curve obtained. The relative experimental error $\Delta l/l$ compared to standard copper is less than $\pm 1\%$ below 20 K and decreases down to 0.3% near 200 K. The samples were cylinders or parallelepipeds (l = 5–6 mm, diameter ~4 mm) with plane-parallel basis (precision $\pm 1\mu$m).

3. Results and discussion

The temperature dependences of the thermal expansion coefficients α for the YB_{12} tricrystal and the LuB_{12} single crystals are shown in figure 4. Both compounds reveal a negative thermal expansion (NTE). In the case of LuB_{12} there are two intervals of NTE: the 'low-temperature' one with a minimum at about 12 K and the 'high-temperature' one with a minimum at about 90 K. The YB_{12} thermal expansion reveals only the 'high-temperature' NTE with a minimum at about 60 K; instead of the 'low-temperature' NTE only an α minimum occurs at ~15 K. The YB_{12} 'high-temperature' NTE anomaly is shifted to lower temperatures in comparison with the LuB_{12} one.

There is a slight difference in the thermal expansion of the LuB_{12} single crystals with $\langle 100\rangle$ and $\langle 110\rangle$ orientations. Because of technical reasons it was impossible to cut two samples along $\langle 100\rangle$ and $\langle 110\rangle$ axes from the same single crystal ingot for the $\Delta l/l$ measurements. The possible origins of the difference in the values of α are (1) high sensitivity of the thermal expansion of LuB_{12} to the quality of the single crystals grown, (2) the anisotropy of the chemical bonds (the $\langle 100\rangle$ axis corresponds to the Me–B bond direction and the $\langle 110\rangle$ axis to the Me–Me bond) and/or (3) the distortion of the LuB_{12} crystal structure at low temperatures from the cubic one. An x-ray study of the LuB_{12} crystal structure down to low temperatures (about 10 K) is in progress.

For these two compounds the coefficient α is a sum of the phonon α_{ph} and electron α_e contributions. The sign of α is determined by the sign of the effective Grüneisen parameter Γ_{eff}

$$\alpha = \Gamma_{eff} C_v / 3BV \tag{1}$$

because the heat capacity at constant volume C_v, isothermal bulk modulus B and molar volume V are positive quantities.

The measured $\Gamma_{\rm eff}$ is the average of the electron $\Gamma_{\rm e}$ and phonon $\Gamma_{\rm ph}$ Grüneisen parameters weighted with the respective heat capacities—the electron ($C_{\rm e}$) and the phonon ($C_{\rm ph}$) ones:

$$\Gamma_{\rm eff} = (\Gamma_{\rm e} C_{\rm e} + \Gamma_{\rm ph} C_{\rm ph})/C_v. \tag{2}$$

Conduction electrons give a contribution to the effective Grüneisen parameter only at low temperatures, when $C_{\rm e}$ becomes comparable with $C_{\rm ph}$. The YB_{12} and LuB_{12} high-temperature NTEs are located in the middle temperature range. So we have supposed that this anomaly is determined by dodecaboride phonon spectra peculiarities.

The phonon Grüneisen parameter $\Gamma_{\rm ph}$ is weighted average of all Γ_i:

$$\Gamma_{\rm ph} = \frac{\sum_i \Gamma_i C_i}{\sum_i C_i} \tag{3}$$

where

$$\Gamma_i = -\frac{{\rm d}\ln \omega_i}{{\rm d}\ln V} \tag{4}$$

is the Grüneisen parameter of the ith frequency mode, the sign of which is determined by the sign of the $\partial\omega_i/\partial V$ derivative and may be both positive and negative; C_i is the heat capacity of the ith mode. As the total $\Gamma_{\rm ph}$ is determined by contributions from all phonon modes, the sign of $\Gamma_{\rm ph}$ may be positive or negative depending on correlation among individual positive and negative Γ_i-value contributions [17].

As we show below, one may obtain the necessary information on low-lying states of the phonon spectra of YB_{12} and LuB_{12} from the temperature dependence of their lattice heat capacity.

The temperature dependence of the heat capacities of both dodecaborides is shown in figure 5. Up to 2.5 K we did not find any evidence of the YB_{12} superconductive transition: the heat capacity in the magnetic field and without it coincided. No transition is seen on the thermogram. It is possible that the superconductive transition detected by Mathias *et al* YB_{12} was induced by YB_6 impurities with $T_{\rm c} = 7.1$ K [2]. There is an additional feature on the YB_{12} heat capacity curve: at low temperatures it is an extremely small value and as a consequence there is data scattering. In order to be sure that the YB12 low-temperature heat capacity, which we analyse in low-temperature model, corresponds to the normal state and not the superconducting one, we have treated the heat capacity data obtained in magnetic field ($H = 1$ T) at $T < 6$ K (figure 5). The heat capacity of YB_{12} and LuB_{12} is a sum of two contributions—the electron ($C_{\rm e}$) and phonon ($C_{\rm ph}$) ones. At low temperatures

$$C_p = \gamma T + bT^3, \tag{5}$$

where γ and b are coefficients of the renormalized electronic heat capacity and of phonon heat capacity, respectively. b is equal to $\{(12/5)r R\pi^4/\Theta_{\rm D}^3\}$ with $r = 13$ being the number of atoms in the molecule of the UB_{12} structure type. From the plot of C_p/T versus T^2 (insets in figure 5) we determined the Sommerfeld coefficient γ and the Debye temperature $\Theta_{\rm D}$. They are equal to 4.13 ± 0.03 mJ mol^{-1}K^{-2} and 1190 ± 70 K for LuB_{12} and 3.11 ± 0.03 mJ mol^{-1} K^{-2} and 1040 ± 15 K for YB_{12}.

The estimated γ-value for LuB_{12} is close to $\gamma \approx 4.2$ mJ mol^{-1} K^{-2} reported by Iga *et al* [18]. The non-renormalized LuB_{12} γ_0-value is equal to 2.85 mJ mol^{-1} K^{-2} [19]. The difference between γ and γ_0 is caused by the enhancement of the effective mass of conduction electrons due to their coupling with phonons [20]. The experimental enhancement factor (the electron–phonon coupling) $\lambda_{\rm ph-e} = (\gamma/\gamma_0) - 1 = 0.45$. We estimated $\lambda_{\rm ph-e}$ using equations

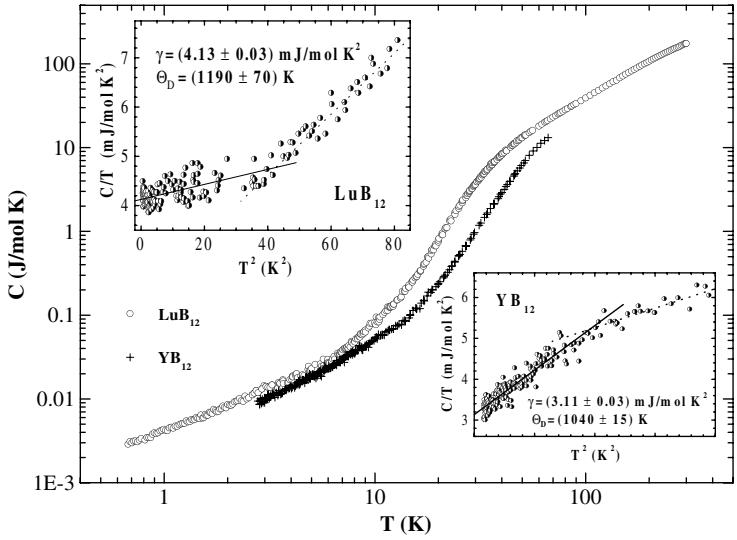

Figure 5. The temperature dependence of the YB_{12} and LuB_{12} heat capacity. Insets: C/T versus T^2 for YB_{12} and LuB_{12}.

obtained for two cases: (a) for the weak-coupling limit and Einstein phonon spectra [21] and (b) for the extended spectrum with a Debye temperature [22]. For the superconducting transition temperature $T_c = 0.4$ K [3] respectively the calculated λ_{ph-e}-values are equal to 0.39 ± 0.05 and 0.35 ± 0.05 for $\mu^* = 0.13 \pm 0.03$ for two characteristic temperatures $\Theta_E = 164$ K (see below) and $\Theta_D = 1190$ K.

For YB_{12}, γ_0 is equal to 2.36 mJ mol^{-1} K^{-2} [19], $\lambda_{ph-e} = 0.32$. As was remarked above, the YB_6 superconducting transition has not been found up to 2.5 K. The estimated λ_{ph-e} are equal to 0.46 or 0.57 for the upper experimental limit $T = 2.5$ K and $\Theta_D = 1040$ K or $\Theta_E = 254$ K respectively and are far from experimental $\lambda_{ph-e} = 0.32$, which is additional evidence that the above-mentioned value $T_c = 4.7$ K is unreal.

The estimated Θ_D for YB_{12} and LuB_{12} are close to Θ_D for β-boron determined by the x-ray method (1250 K) [12] and calculated from the elastic constants (1370 K) [23], which suggests that the strengths of the bonding in these solids are similar. Unfortunately, a large scattering of experimental points in the low-temperature range due to the very small heat capacity of LuB_{12} did not allow us to determine its Θ_D-value more accurately.

For both compounds C_p/T versus T^2 plots reveals a knee at low temperatures (insets in figure 5). Such behaviour of C_p was found also for rare earth hexaborides [24]. Takegahara and Kasuya [25] supposed that such an anomaly in the hexaboride case is due to the defect-induced soft mode. Calculations of the LaB_6 heat capacity from its point contact (PC) spectra, which included a zero bias anomaly usually connected with impurities and defects, gave a similar knee in the C_p/T versus T^2 plot [26] confirming Takegahara and Kasuya's idea.

Now we try to extract information on the phonon spectra of yttrium and lutetium dodecaborides from their heat capacities.

According to Junod *et al* [27], $5/4R\pi^4 C_{ph}/T^3$ versus (T (1 K)) gives an approximate picture of the one-dimensional phonon density of states $\omega^{-2}F(\omega)$ for $\omega = 4.928T$, where ω is expressed in kelvins. On a logarithmic scale the response of C_{ph}/T^3 to a δ function (Einstein peak) is a bell-shaped peak.

Table 1. The frequencies of the LuB_{12} Raman modes (meV).

Modes					
F_{2g}	E_g	F_{2g}	E_g	A_g	Ref.
56.34	83.42	102.6	125.8	134.6	[7]
	82.20	97.20		129.3	[9]

Table 2. The Einstein frequencies (Θ_{E_i}) for LuB_{12}.

	Heat capacity (this work)			Neutron [6]		PC spectrum [8]	
Nos	K	meV	Degeneracy	K	meV	K	meV
1	58.0	4.9	0.049			(31.3)[a]	(2.7)
2	163.7	14.1	3	164.8	14.2	168.3 (163.6)	14.5 (14.1)
3	307.5	26.5	2	273.2	23.6	280.8	24.4
4	374.4	32.3	1	374.6	32.3	338.9	29.2
5	513.0	44.2	3	491.3	42.4	436.3	37.6
6	743.0	64.0	3	579.5	49.9		
7	843.0	72.64	3				
8	990.0	85.31	3				
9	1405.0	121.0	7				

[a] The energies in brackets from the PC spectra are obtained for high-resistance contacts; the other ones are for low-resistance contacts [8].

After elimination of the electron heat capacity ($C_e = \gamma T$, $\gamma = \text{const}$) such an analysis of the phonon heat capacity ($C_{ph} = C_p - C_{el}$) was carried out for both compounds. We have found well-defined bell-shaped peaks, with maxima corresponding to the phonon modes with characteristic energies of ($\omega_E \approx 5T_m$) about 14.0 and 22 meV for LuB_{12} and YB_{12}, respectively (figures 6(a), (b)—circles). The obtained energy of about 14 meV for LuB_{12} agrees with the flat mode from free vibrations of the Lu ion obtained from the neutron and PC spectra [6, 8] (table 2).

By analogy with results for LaB_6 [28], we consider the molecule of UB_{12} structure type as a diatomic molecule, where one atom is the metal and other is the B_{12} structure unit, and calculated the heat capacity of LuB_{12} as a superposition of electron (C_{el}), Debye (C_D) and single Einstein (C_E) contributions. We linked the Debye heat capacity with the B sublattice and calculated it for 12 moles of the B ions; the Einstein heat capacity was attributed to the metal sublattice and respectively to 1 mol of the Lu ions. For these calculations we used the specific Θ_D-value from the C_p/T versus T^2 plot.

The value of Θ_E was found from the peak value of the C_{ph}/T^3 versus $\ln(T/K)$ curve.

The experimental and calculated LuB_{12} heat capacities show satisfactory agreement; however, the existence of a structure in the remainders $\{[C_p(\text{exp}) - C_p(\text{cal})]/C_p(\text{exp}) \cdot 100\%\}$ (figure 7(a)) testifies that the agreement is only apparent, and correspondingly the given model is inadequate to explain the experimental data. The strongest disagreement is observed for the low-energy part. a similar C_p behaviour is observed for YB_{12} (figure 7(b)).

The solution of the inverse task—the reconstruction of the phonon spectrum from the heat capacity—is a very difficult problem. For a molecule having 13 atoms, such as the dodecaboride one, in the case of completely lifted degeneracy the number of modes has to be equal to 39; three acoustic modes are related with the Debye contribution to the heat capacity, and the remaining optic ones are Einstein contributions. For LuB_{12} the values of its five high-energy modes ($2F_g$, $2E_g$, A_g) are known from its Raman spectra (table 1) [7, 9]; accounting for their degeneracy we still have 11 modes.

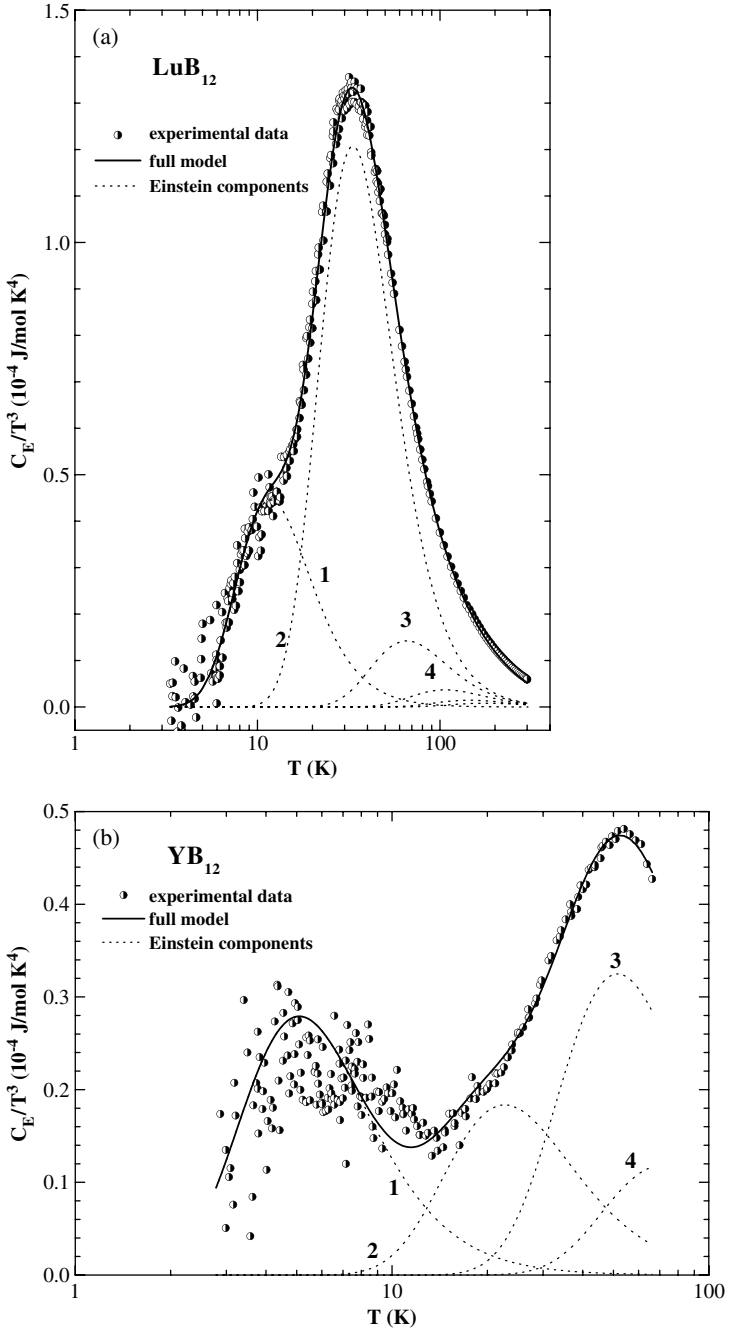

Figure 6. $C_{\rm ph}/T^3$ versus $\log T$ for LuB_{12} (a) and YB_{12} (b). The circles are experimental data, and the lines are fitted curves. For LuB_{12} the symbols (1–4) correspond to the next energies of the Einstein modes, 58.0, 163.7, 307.5, 374.4 K; for YB_{12} the symbols (1–4) correspond to energies 25.5, 111.4, 254, 359.7 K.

In order to evaluate the remaining 25 modes, some of which may be degenerated, we subtracted Raman and Debye contributions from the LuB_{12} full phonon heat capacity and

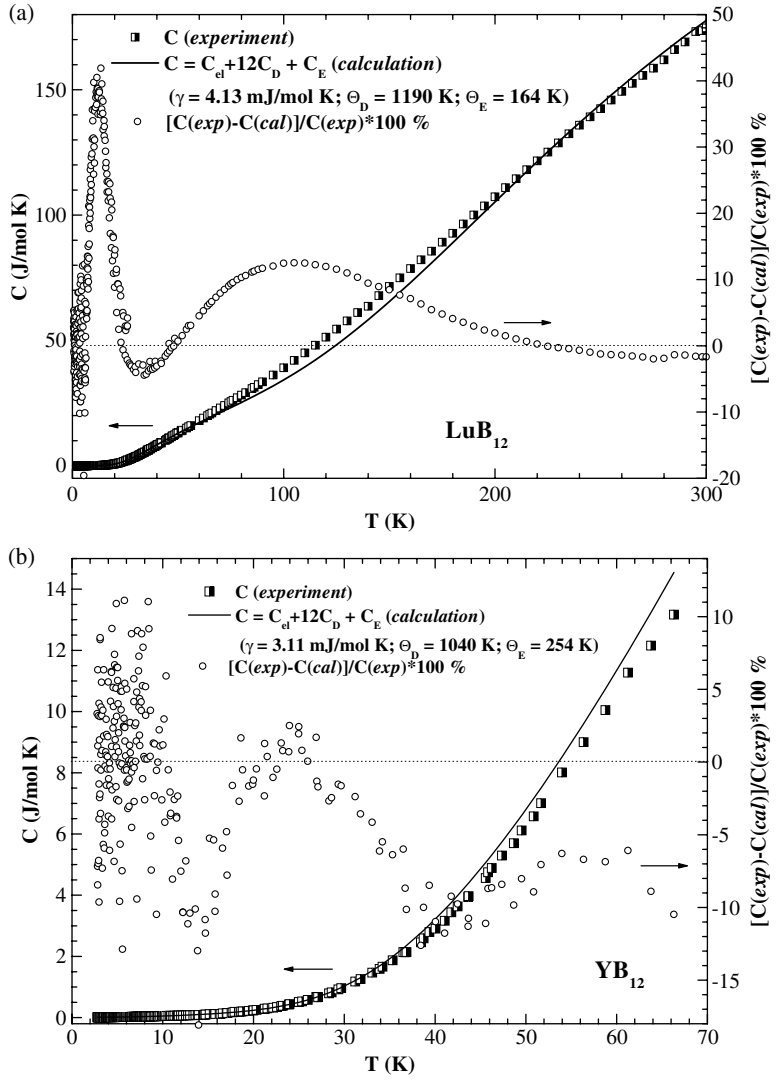

Figure 7. The temperature dependence of the experimental and calculated (using the model of a bi-atomic molecule; see the text) MeB_{12} heat capacity and of the relative error between them: (a) LuB_{12}, (b) YB_{12}.

fitted the remaining heat capacity (C_E) by a set of Einstein components (Θ_{E_i}). The results of this fitting are presented in figure 6(a) and table 2; in the latter the data from neutron experiment and PC spectra are also presented. Taking into account that on this scale only the contribution of low-lying modes is clearly seen, in figure 8 all components are presented on the usual scale $C = f(T)$ in order to evaluate their contribution to the heat capacity in different temperature ranges.

The agreement between experimental and fitted Θ_{E_i}-values (table 2) for the low-energy modes is satisfactory; it is necessary to consider the values of high-energy modes as estimates. Any divergence of the modes from the PC spectra may be attributed to the anisotropy of the LuB_{12} phonon spectrum which is known to exist for the other boride, LaB_6 [26]. Unfortunately

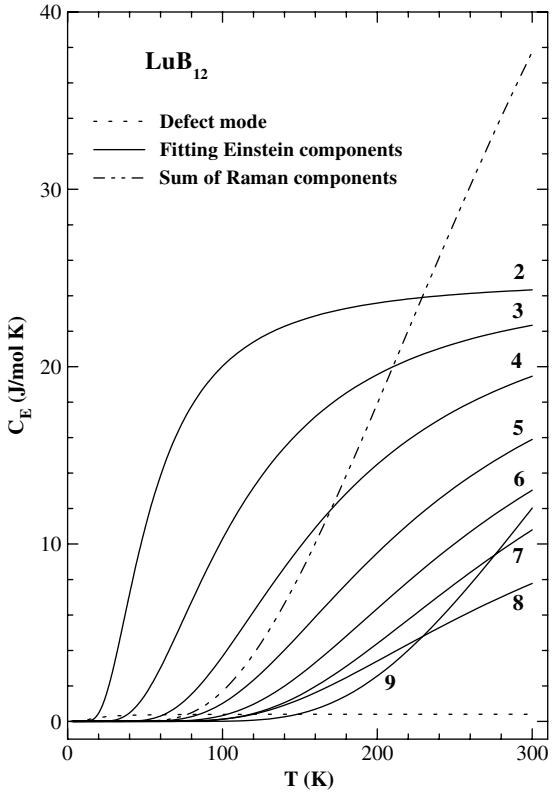

Figure 8. The temperature dependences of contributions of the individual Einstein phonon modes to the LuB_{12} heat capacity. The numbers at the curves correspond to the numbers of the Einstein components in table 2.

information on the LuB_{12} PC spectrum is presented only for a unique orientation of the sample [8]. Spectra obtained from data on the neutron scattering and heat capacity are averaged ones, in contrast to the PC spectra.

Let us examine the information from figure 6(a).

In order to obtain the best fitting in the low-energy part of the LuB_{12} heat capacity we introduced an additional Einstein contribution with a small weight (∼0.05) and energy ∼4.9 meV (figure 6(a), table 2). This contribution to C_{ph} is very small in general but very essential at low temperatures. The calculations of the electron heat capacity for the Grimvall model [29] leads to similar results[6]. This low-energy mode corresponds to the zero-bias anomaly in the PC spectrum (table 2). So, we assume that it is a defect-induced soft mode, and that the 'low-temperature' NTE and the anomalous low-temperature dependence of the LuB_{12} heat capacity have the same origin—a possible formation of the two-level tunnelling system based on the metal ions and defects [25]. Earlier, an identical mechanism has been proposed for the explanation of the low-temperature NTE in LaB_6 single crystals [30].

[6] Grimvall presented the calculated temperature dependence of the electron–phonon renormalization contribution $\gamma_{ep}(T)/\gamma_{ep}(0)$ to the electronic heat capacity as a plot. The calculation was done for an Einstein phonon spectrum. The temperature dependence is non-monotonic; its distinguishing feature is the peak $\gamma_{ep}(T)/\gamma_{ep}(0)$ at a low temperature, such as $T/\theta_E \sim 0.1$. Taking into account the relatively small energy of the first Einstein mode we wanted to exclude the possible effect of the electron heat capacity's nonlinear character.

The main contribution to C_{ph} for LuB_{12} at low temperatures is related to the mode equal to 14.1 meV (figure 6(a)) that is very close to the energy of the δ-like peak from the neutron phonon spectrum (14.2 meV) [6] and from the PC spectrum (14.5 meV) [8]. The use of this phonon mode resulted in the estimate $\lambda_{ph-e} = 0.39$ from the equation for T_c in the weak-coupling limit and for Einstein phonon spectra [21]. This value is close to the experimental value $\lambda_{ph-e} = 0.45$; however, to say unambiguously that the electron–phonon coupling constant λ_{ph-e} is determined first of all by the interaction of electrons with the low-energy first mode in the phonon spectrum is impossible, as $\lambda_{ph-e} = 0.35$ from the formula for extended spectrum with a Debye temperature [22] has a similar value.

The LuB_{12} phonon spectrum from [6, 8] is very similar to that for LaB_6 [25, 31], in which the first δ-like peak at 12.4 meV corresponds to the flat acoustic longitudinal and transverse modes in the larger part of the first Brillouin zone. It is supposed that the flattening of LaB_6 dispersion curves is connected with vibrations of the non-interacting La ions. The distance between the metal atoms in LuB_{12} is about 20% larger than in LaB_6 and so the Me–Me bond is weaker in it. Therefore one may assume that acoustic phonon branches for LuB_{12} have a similar form as the LaB_6 ones.

We extended this assumption to the YB_{12} phonon spectrum. For YB_{12} we had the heat capacity data only up to 70 K. The absence of information on the YB_{12} high-energy Raman active modes has been no barrier for deconvolution of its phonon heat capacity to the phonon spectrum as these modes are related to the intramolecular B–B vibrations and have to be similar for both compounds. The evaluation of their contribution to the YB_{12} C_{ph} in this temperature range has shown that it is negligible. Results of deconvolution are presented in figure 6(b). By analogy with LuB_{12} we related the mode at 21.9 meV (254 K) with free vibrations of yttrium atoms in the boron cavities. The value of the higher-energy mode is equal to ~31 meV with degeneracy 3. However, for more correct fitting of the low-energy part of the spectrum we had to include two additional modes—2.2 and ~9.6 meV with weights 0.0025 and 0.14, respectively. We suppose that they have the same nature as the mode with energy ~4.9 meV for LuB_{12}.

One can explain the softening of the LuB_{12} phonon at 14.1 meV in comparison with the YB_{12} one at 21.9 meV in the following manner. The 17% difference in the Y and Lu ion radius (0.97 and 0.80 Å relatively) corresponds to the ~0.5% difference in the YB_{12} and LuB_{12} lattice parameters (7.500_1 and 7.4644_2 Å, respectively). So the decreasing of the radius of the metal ion located in the centre of the Fedorov cubooctahedron should lead to weakening of the Lu–B bond, certain destabilization of the lattice, softening of the Lu-phonon mode and larger LuB_{12} heat capacity than that of YB_{12}.

In a first approximation the electron–phonon coupling λ_{ph-e} is proportional to the vibration amplitude of the metal $(\hbar/2M_{Me}\omega_{Me})^{1/2}$, where M_{Me} and ω_{Me} are the mass and phonon frequency of the metal. The calculation of the Y and Lu metal vibrational amplitudes in both compounds gives close values for their experimental M_{Me} and ω_{Me}, which agrees with the fact that both λ_{ph-e}-values are close to that estimated from McMillan's formula (0.40 and 0.43 relatively) for Θ_{Ei} equal to 21.9 meV (YB_{12}) and 14.1 meV (LuB_{12}) and the same $T_c = 0.4$ K. This fact also gives evidence that the $T_c = 4.7$ K for YB_{12} obtained by Matthias *et al* [2] is in error.

The existence of the negative Γ_i for the dispersion-free transverse acoustic phonon modes was predicted for the first time by Dayal [32] and Barron [33]. The prevailing negative contribution of their Γ_i to the general phonon Grüneisen parameter results in the negativity of Γ_{ph} in definite temperature ranges even for such simple substances as tetrahedral semiconductors Si and Ge [32–35 and references cited therein]. Taking into account the possible dispersionless character of the YB_{12} and LuB_{12} low-energy phonon modes we suppose

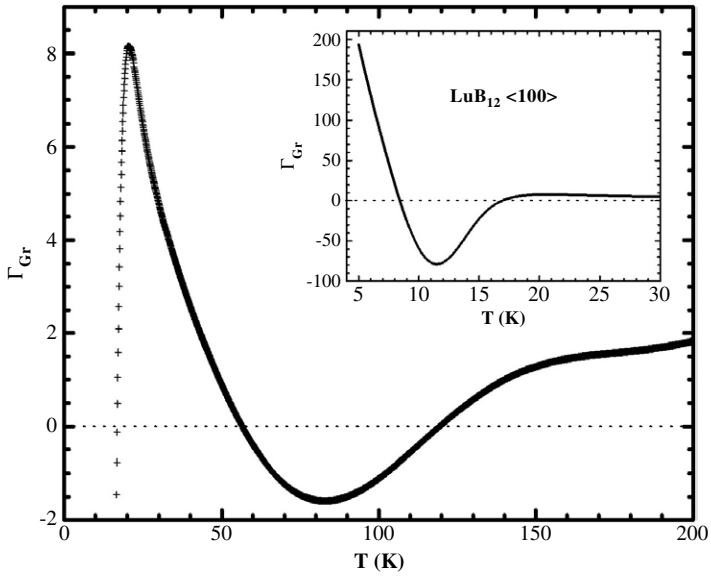

Figure 9. The LuB_{12} generalized Grüneisen parameter Γ_{Gr}. Inset: Γ_{Gr} versus T for LuB_{12} in the expanded low-temperature scale 5–30 K.

that their 'high-temperature' NTEs are caused by the negative partial contribution Γ_i from the transverse acoustic modes to a generalized Grüneisen parameter Γ_{Gr}. For temperatures at which excitations of the transverse phonons with short wavelengths and negative partial contributions Γ_i will dominate, one would expect the NTE.

Due to the alternating signs of the partial Grüneisen parameters and peculiarities in the phonon spectra at 4.2–300 K, the Si and Ge lattice parameters and consequently the thermal expansion coefficients weakly depend on temperature [34]. We think that the small α-values of dodecaborides are explained by similar reasons in addition to the role of the rigid boron sublattice.

On the ground of the experimental heat capacity, thermal expansion and bulk modulus (c_B) data we evaluated the temperature dependence of the LuB_{12} generalized Grüneisen parameter Γ_{Gr}. In figure 9, Γ_{Gr} is presented for $LuB_{12}\langle 100\rangle$. In the 10–20 and 60–120 K ranges Γ_{Gr} for LuB_{12} is negative in accordance with its two ranges of NTE, whereas the LuB_{12} C_p from 5 K up to 200 K is a monotonically increasing function of temperature (figure 5) and c_B is a smooth monotonically decreasing function of temperature from 229.5 up to 224.9 GPa, respectively. As a result, the generalized Grüneisen parameter Γ_{Gr}, but not the heat capacity, mainly determines the LuB_{12} $\alpha(T)$ behaviour. As c_B and C_p for both LuB_{12} samples are the same, the Γ_{Gr} general structure (two negative minima) is the same for both orientations according to the α behaviour; the difference between two Γ_{Gr} is only in details—in the positions of minima and in the Γ_{Gr} absolute values at the same temperatures. For YB_{12} the Grüneisen parameter was not calculated, due to the absence of the bulk modulus data.

We make a last remark. Let us consider a possible mechanism responsible for flattening of the low-lying acoustic branches. Based on the experimental facts, we supposed that the metal ions freely vibrate as harmonic oscillators in the cavities of the boride sublattice. That is, the metal ions behave as a concentrated impurity with a quasi-local frequency. Kossevic [36] considered the behaviour of such a system and concluded that even a small interaction between vibrations of two subsystems results in two branches of the spectrum

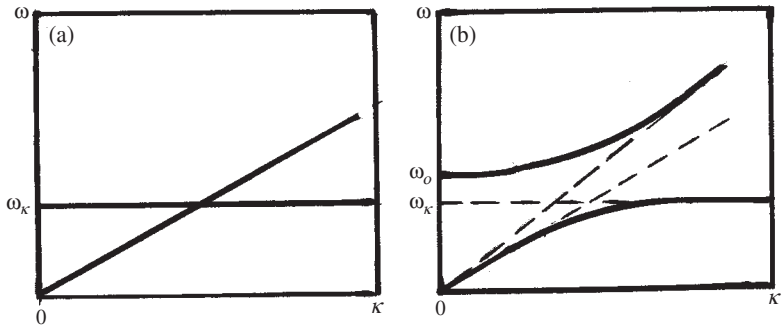

Figure 10. A schematic diagram of the phonon dispersion law for a crystal with large impurity concentration: (a) the intersection of the sound dispersion law with the quasi-local frequency of homogeneously distributed impurities; (b) two branches of long-wave vibrations divided by a quasi-gap [36].

of the long-wave vibrations. In figure 10 the scheme of the phonon dispersion law for a crystal with a large impurity concentration is presented: it shows the intersection of the sound dispersion law ($\omega = s_0 k$) with the quasi-local frequency of a homogeneously distributed impurity ($\omega = \omega_k = \text{const}$) (figure 10(a)) and formation of two phonon branches with a quasi-gap due to removing of a hypothetical degeneration of frequencies (figure 10(b)) [36]. Under such an approach the formation of flat pieces of dispersion curves in the largest part of the first Brillouin zone becomes clear, and one may comment on deformation of the long-wave range of the phonon spectrum.

4. Conclusion

We studied the thermal expansion and heat capacity of non-magnetic yttrium and lutetium dodecaborides in the low and middle temperature intervals and found the ranges of the negative thermal expansion for both compounds at definite temperatures. The 'low-energy' NTE is connected with the possible formation of a two-level tunnelling system based on the metal ions and lattice defects. The NTE at middle temperatures is explained by the features of the phonon structure of these compounds: the flat transverse acoustic phonon modes in the superior part of the first Brillouin zone that results in the negative partial contribution of the Grüneisen parameters Γ_i of these modes to the generalized Grüneisen parameter Γ_{Gr}. The existence of such modes follows from the heat capacity analysis. They appear as a result of oscillations of the non-interacting metal ions in the cavities of the boron sublattice.

Acknowledgments

We should like to thank I Kolobov for providing data on LuB_{12} bulk modulus. This work has been in part supported under the INTAS Project, Ref. No. 03-51-3036.

References

[1] Matkovich V I and Economy J 1977 *Boron and Refractory Borides* ed V I Matkovich (Berlin: Springer) p 78
[2] Matthias S T, Geballe T H, Andres K, Corenzwit E, Hull G W and Maita J P 1968 *Science* **159** 530

[3] Batko I, Batkova V, Flachbart R, Paderno Y B, Filippov V, Shitsevalova N Y and Wagner T H 1995 *J. Alloys Compounds* **217** L1
[4] Kasaya M, Iga F, Takigawa M and Kasuya T 1985 *J. Magn. Magn. Mater.* **47/48** 429
[5] Czopnik A, Shitsevalova N, Krivchikov A, Pluzhnikov V, Paderno Yu and Onuki Y 2004 *J. Solid State Chem.* **177** 507
[6] Bouvet A, Kasuya T, Bonet M, Regnault L P, Rossat-Mignod J, Iga F, Bak B and Severing A 1998 *J. Phys.: Condens. Matter* **10** 5667
[7] Fujita Y, Ogita N, Shimizu N, Iga F, Takabatake T and Udagawa M 1999 *J. Phys. Soc. Japan* **68** 4051
[8] Flachbart K, Samuely P, Szabo P, Gloos K, Paderno Y and Shitsevalova N 2002 *Czech. J. Phys.* **52** (Suppl. A) 221
[9] Werheit H, Paderno Y, Filippov V, Paderno V, Shwartz U and Pietraszko A 2004 *Proc. Conf. on Materials and Coatings for Extreme Performances: Investigations, Applications, Ecologically Safe Technologies for their Production and Utilization* ed V V Skorokhod (Kiev: IPMS) p 520
[10] Paderno Y, Odintsov V V, Timofeeva I I and Klochkov L A 1971 *Thermal Phys. High Temp.* **9** 200 (in Russian)
[11] Dutczak Ya I, Fedyshin Ya I, Paderno Y B and Vadetz D I 1972 *Elektronn. Tekhn.* 6 **4** 120 (in Russian)
[12] Moiseenko L L 1980 *Sov. Powder Metall.* **7** 100 (in Russian)
[13] Johnson R W and Daane A H 1963 *J. Chem. Phys.* **38** 425
[14] Krivchikov A I, Gorodilov B Ya and Czopnik A 1997 *Proc. Conf. on Low Temperature Thermometry and Dynamic Temperature Measurements* (Wrocław: ILTSR) p V7
[15] Yachmenev V E, Movchan N P, Dudnik E M and Kolesnikova E A 1978 *Sov. Powder Metall.* **6** 75 (in Russian)
[16] Brandli G and Griessen R 1973 *Cryogenics* **13** 299
[17] Barron T H K, Collins J G and White G K 1980 *Adv. Phys.* **29** 609
[18] Iga F, Kasaya M and Kasuya T 1988 *J. Magn. Magn. Mater.* **76/77** 156
[19] Harima H, Yanase A and Kasuya T 1985 *J. Magn. Magn. Mater.* **47/48** 567
[20] Fulde P and Jensen J 1983 *Phys. Rev.* B **27** 4085
[21] Combescot R 1990 *Phys. Rev.* B **42** 7810
[22] Allen P B and Dynes R C 1975 *Phys. Rev.* B **12** 905
[23] Silverstova I M, Belayev L M and Pisarevski Y V 1974 *Mater. Res. Bull.* **9** 1101
[24] Etourneau J, Mercurio J-P, Naslain R and Hagenmuller P 1970 *J. Solid State Chem.* **2** 332
[25] Takegahara K and Kasuya T 1985 *Solid State Commun.* **53** 21
[26] Samuely P, Reiffers M, Flachbart K, Akimenko A I, Yanson I K, Ponomarenko N M and Paderno Yu B 1988 *J. Low Temp. Phys.* **71** 49
[27] Junod A, Jarlborg T and Muller J 1983 *Phys. Rev.* B **27** 1568
[28] Mandrus D, Sales B C and Jin R 2001 *Phys. Rev.* B **64** 012302
[29] Grimvall G 1981 *The Electron–Phonon Interaction in Metals* (Amsterdam: North-Holland)
[30] Pluzhnikov V B 2000 private communication
[31] Smith H G, Dolling G, Kunii S, Kasaya M, Liu B, Takegahara K, Kasuya T and Goto T 1985 *Solid State Commun.* **53** 15
[32] Dayal B 1944 *Proc. Indian Acad. Sci.* A **20** 145
[33] Barron T H K 1955 *Phil. Mag.* **46** 720
[34] Novikova S I 1979 *Thermal Expansion of Solid States* (Moscow: Nauka) (in Russian)
[35] Jernov A P 2000 *Low Temp. Phys.* **26** 908
[36] Kossevich A M 1999 *The Crystal Lattice: Phonons, Solitons, Dislocations* (Berlin: Wiley–VCH)